Preprints (www.preprints.org) | NOT PEER-REVIEWED | Posted: 1 March 2021 doi:10.20944/preprints202103.0021.v1

Ultra-large Optical Kerr Nonlinearity in 2D $PdSe_2$ Dichalcogenide Thin Films for Integrated Nonlinear Photonics

Linnan Jia, Jiayang Wu, David J. Moss

[a]*Optical Sciences Centre, Swinburne University of Technology, Hawthorn, VIC 3122, Australia*

* E-mail: dmoss@swin.edu.au

ABSTRACT

As a novel layered noble metal dichalcogenide material, palladium diselenide ($PdSe_2$) has attracted wide interest due to its excellent optical and electronic properties. In this work, a strong third-order nonlinear optical response of 2D $PdSe_2$ films is reported. We conduct both open-aperture (OA) and closed-aperture (CA) Z-scan measurements with a femtosecond pulsed laser at 800 nm to investigate the nonlinear absorption and nonlinear refraction, respectively. In the OA experiment, we observe optical limiting behaviour originating from large two photo absorption (TPA) in the $PdSe_2$ film of β = 3.26 $\times 10^{-8}$ m/W. In the CA experiment, we measure a peak-valley response corresponding to a large and negative Kerr nonlinearity of $n_2 = -1.33\times10^{-15}$ m^2/W – two orders of magnitude larger than bulk silicon. In addition, the variation of n_2 as a function of laser intensity is also characterized, with n_2 decreasing in magnitude when increasing incident laser intensity, becoming saturated at $n_2 = -9.96\times10^{-16}$ m^2/W at high intensities. Our results show that the extraordinary third-order nonlinear optical properties of $PdSe_2$ have strong potential for high-performance nonlinear photonic devices.

Keywords: 2D materials, $PdSe_2$ films, Z-scan technique, Kerr nonlinearity, nonlinear photonics.

1. INTRODUCTION

Two-dimensional (2D) layered materials such as graphene, [1-3] graphene oxide (GO), [4-9] transition metal dichalcogenides (TMDCs), [10-12] and black phosphorus (BP) [13,14] have attracted a great deal of interest, enabling diverse nonlinear photonic devices with vastly superior performance compared to bulk materials. Amongst them, TMDCs (MX_2, M = transition metal and X = chalcogen), with bandgaps in the near infrared to the visible region, have opened up promising new avenues for photonic and optoelectronic devices. [2,15,16] For instance, a few mono-layers of MoS_2 and WS_2 have been used as broadband, fast-recovery saturable absorbers for mode locking in pulsed fiber lasers. [2,15] Nonlinear optical modulators and polarization dependent all-optical switching devices have been realized based on $ReSe_2$ [16] and SnSe. [17] As a new 2D noble metal dichalcogenide in the TMDC family, $PdSe_2$ has recently attracted significant interest. [18-21] Similar to the puckered structure of BP, it has a puckered pentagonal atomic structure − with one Pd atom bonding to four Se atoms and two adjacent Se atoms covalently bonding with each other. Due to this low-symmetry structure, $PdSe_2$ possesses unique in-plane anisotropic optical and electronic properties, [18,19] featuring an in-plane noncentrosymmetric structure, in contrast to its cousin $PtSe_2$. Further, $PdSe_2$ has a layer-dependent bandgap, varying from 0 eV (bulk) to 1.3 eV (monolayer) - a property well suited for photonic and optoelectronic applications – in particular, for wavelength tuneable devices. Moreover, different to BP which degrades rapidly under ambient conditions, $PdSe_2$ is highly air-stable, indicating its robustness and potential for practical applications. The high carrier mobility and anisotropic Raman spectroscopy of 2D $PdSe_2$ layers have been investigated [18,20] as well as highly-sensitive photodetectors from the visible to mid-infrared wavelengths. [22,23] Recently, the optical nonlinear absorption of $PdSe_2$ nanosheets has also been reported in the context of mode-locked laser applications. [24,25] To date, however, its optical Kerr nonlinearity has not been investigated.

Here, we characterize the third-order nonlinear optical properties of $PdSe_2$ multilayer films via Z-scan technique with femtosecond optical pulses at 800 nm. Both OA and CA measurements are performed to investigate the nonlinear absorption and nonlinear refraction of $PdSe_2$. Experimental results show that $PdSe_2$ films exhibit a large and negative (self-defocusing) Kerr nonlinearity (n_2) of ~ -1.33×10^{-15} m^2/W, two orders of magnitude larger than bulk silicon. In the OA measurement, we observe a large nonlinear absorption β of ~ 3.26 $\times 10^{-8}$ m/W, which originates from TPA in the $PdSe_2$ films. In addition, we investigate the intensity dependence of the nonlinear response of $PdSe_2$, finding that the absolute magnitude of the Kerr nonlinearity n_2 initially decreases slightly with incident laser intensity, becoming saturated at higher intensities. These results verify the large third-order nonlinear optical response of $PdSe_2$ as well as its strong potential for high-performance nonlinear photonic devices.

Preprints (www.preprints.org) | NOT PEER-REVIEWED | Posted: 1 March 2021 doi:10.20944/preprints202103.0021.v1

2. MATERIAL PREPARATION AND CHARACTERIZATION

The atomic structure of $PdSe_2$ crystals is shown in Figure 1(a). $PdSe_2$ exhibits a unique puckered pentagonal structure, different to other TMDCs like MoS_2 and WS_2. The Se-Pd-Se layers stack with weak van der Waals interactions to form a layered structure. [18,19] In each monolayer, the pentagonal rings are formed with one Pd atom bonding to four Se atoms and two adjacent Se atoms covalently bonding with each other, which is similar to the puckered structure of BP, and yields both anisotropic and non-centrosymmetric properties of $PdSe_2$. More importantly, unlike the rapid degradation of BP under ambient conditions, $PdSe_2$ has significantly better air-stability. [22,23] Together, these properties of $PdSe_2$ make it promising for high performance photonic and optoelectronic applications.

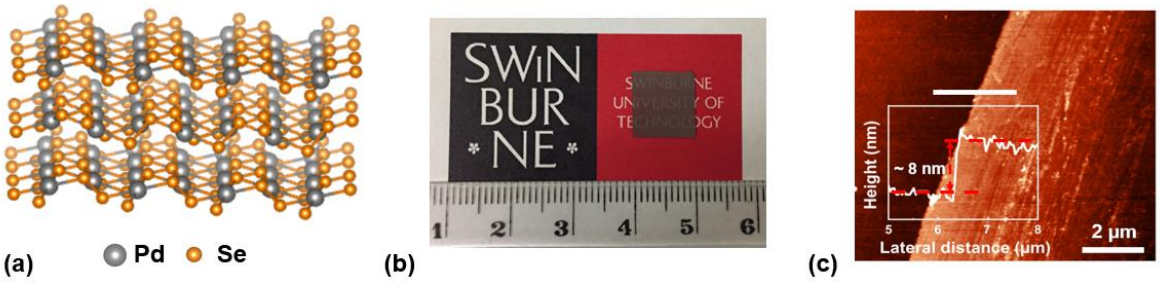

Figure 1. (a) Crystal structure of $PdSe_2$. (b) Photograph of prepared multilayer $PdSe_2$ film. The unit for the numbers on the ruler is centimeter. (c) AFM height profile of the multilayer $PdSe_2$ film.

Here, we investigate large-area multilayer $PdSe_2$ films deposited on transparent sapphire substrates. The $PdSe_2$ films were synthesized via Chemical vapor deposition (CVD). [26] The films were polycrystalline, as is typical for CVD synthesized films, with crystal sizes varying from 10's of nanometres up to 100 nm. Because of the polycrystalline nature of the films, the inversion symmetry breaking properties (i.e., non-centrosymmetric) of the single $PdSe_2$ crystals could not be observed on optical wavelength scales in the macroscopic $PdSe_2$ continuous films studied in this work. Figure 1(b) shows the photography of the prepared $PdSe_2$ film. The morphology image and height profile of the prepared $PdSe_2$ films were characterized by atomic force microscopy (AFM), as illustrated in Figure 1(c). The film thickness was measured to be ~ 8 nm, which corresponds to ~20 layers of $PdSe_2$. [19,26]

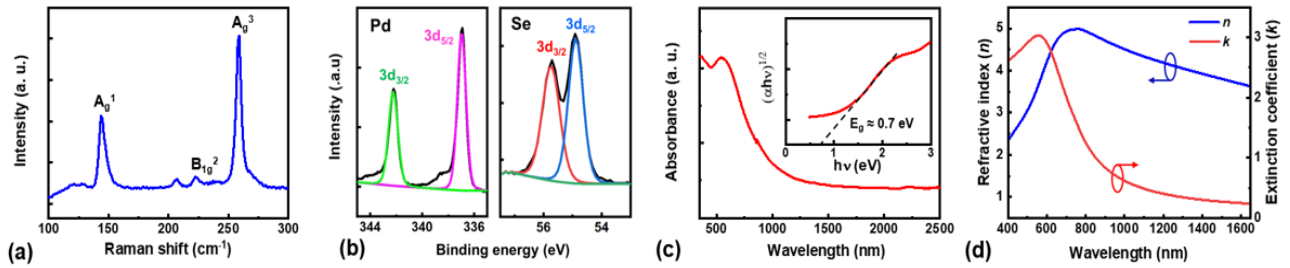

Figure 2. Characterization of the prepared $PdSe_2$ film. (a) Raman spectrum excited via a 514-nm laser. (b) X-ray photoelectron spectroscopy (XPS) spectra. (c) UV-vis absorption spectrum. Inset shows the extracted Tauc plot. (d) Measured refractive index (n) and extinction coefficient (k).

Raman spectrum of the prepared $PdSe_2$ film excited with a laser at 514 nm is shown in Figure 2(a). Three representative phonon modes can be observed, including the A_g^1 (~145.5 cm^{-1}) and B_{1g}^2 (~222.5 cm^{-1}) vibrational modes that correspond to the movement of Se atoms and the A_g^3 (~ 258.8 cm^{-1}) mode that relates to the relative movements between Pd and Se atoms. [20,26] To further characterize the film quality, X-ray photoelectron spectroscopy (XPS) was employed to measure the binding energy of $PdSe_2$. Figure 2(b) shows the XPS results of Pd 3d and Se 3d core levels for the $PdSe_2$. The peaks of the fit at ~ 342.2 eV and ~ 336.9 eV are attributed to the Pd $3d_{3/2}$ and Pd $3d_{5/2}$, respectively, whereas the peaks at ~ 55.7 eV and ~ 54.9 eV correspond to Se $3d_{3/2}$ and $3d_{5/2}$, respectively. [20,26] To characterize the linear absorption and optical bandgap, the optical absorption spectrum (from 400 nm to 2500 nm) of the $PdSe_2$ film was measured with ultraviolet-visible (UV-vis) spectrometry, as shown in Figure 2(c). The inset of Figure 2(c) shows the Tauc plot extracted from the linear absorption spectrum, where the optical bandgap of the $PdSe_2$ film is estimated to be ~ 0.7 eV. We also characterize the in-plane (TE-polarized) refractive index (n) and extinction coefficient (k) of the $PdSe_2$ film via spectral ellipsometry, as depicted in Figure 2(d). The refractive index first increases dramatically with wavelength to reach a peak at ~ 700 nm

Preprints (www.preprints.org) | NOT PEER-REVIEWED | Posted: 1 March 2021 doi:10.20944/preprints202103.0021.v1

and then decreases more gradually at longer wavelengths. The extinction coefficient exhibits a significant decrease from 600 nm to 1200 nm, and then the rate of decrease slows down at longer wavelengths. This shows an agreement with the trend of the UV-vis absorption spectrum in Figure 2(c).

3. Z-SCAN MEASUREMENTS

To investigate the third-order nonlinear optical properties of $PdSe_2$, we characterized the nonlinear absorption and refraction of the prepared $PdSe_2$ films via the Z-scan technique, [27-29] where a femtosecond pulsed laser with a centre wavelength at ~800 nm and pulse duration of ~ 140 fs was used to excite the samples. A half-wave plate combined with a linear polarizer was employed to control the power of the incident light. A beam expansion system consisting of a 25-mm concave lens and 150-mm convex lens was used to expand the light beam, which was then focused by an objective lens (10 ×, 0.25 NA) to achieve a low beam waist with a focal spot size of ~1.6 μm. The prepared samples were oriented perpendicular to the beam axis and translated along the Z-axis with a linear motorized stage. A high-definition charge-coupled-device (CCD) imaging system was used to align the light beam to the target sample. Two photodetectors (PDs) were employed to detect the transmitted light power for the signal and reference arms.

Figure 3(a) shows the OA Z-scan results for the $PdSe_2$ film at three representative intensities. A typical optical limiting behaviour was observed in the OA curves, with the transmission decreasing as the $PdSe_2$ sample was moved through the focal point. We measured the response of pure sapphire substrate and did not observe any significant nonlinear absorption, indicating that the observed optical limiting response was induced by the $PdSe_2$ film. We also note that the transmittance dip of the OA curve decreased when the incident laser intensity was increased. In principle, the optical limiting behaviour can be induced by several mechanisms such as nonlinear light scattering (NLS), reverse saturable absorption (RSA), two-photon absorption (TPA) and multi-photon absorption (MPA). [30,31] However, apart from the basic condition that the total energy of the photons involved in each process (eg., two photons, for TPA, one photon for SA etc.) must be larger than the bandgap, there is no a-priori reason for any particular process to dominate. For thin $PdSe_2$ film in our case, though, we first exclude the NLS effect since it usually dominates for dispersion or solution samples with laser-induced microbubbles. [30,31] According to the UV-vis spectra, the bandgap of the few-layer $PdSe_2$ film is estimated to be 0.7 eV, which is lower than a single photon energy of the incident laser at 800 nm. Therefore, all the above processes can occur. While SA at low laser intensities and RSA at high laser intensities might be expected for the Z-scan measurements, we did not observe this. This could possibly be because the single photon transition is inefficient under 800-nm femtosecond laser excitation due to the indirect band structure of the few-layer 8-nm-thick $PdSe_2$ films, or possibly parallel band absorption effects. [31] Considering this, RSA is unlikely to dominate the nonlinear absorption in $PdSe_2$ films due to its one photon process. Given the high peak power of the incident femtosecond pulses, TPA is likely to account for the optical limiting behaviour observed in our Z-scan measurements.

To extract the TPA coefficient β of $PdSe_2$, we fit the measured OA results with the well-established theory. [27,28] The TPA coefficient β for the $PdSe_2$ film is shown in Figure 3(b) at different laser intensities. A large $\beta = 3.26 \times 10^{-8}$ m/W is observed, which is comparable to the reported values of graphene, and higher than that of WS_2, highlighting the strong optical limiting effect in $PdSe_2$ film. In addition, the TPA coefficient β is relatively constant with incident laser intensity, reflecting the fact that we are working in an intensity regime where the material properties of the $PdSe_2$ films are not changing much. The slight fluctuation in β with laser intensity may arise from light scattering in the $PdSe_2$ film surface.

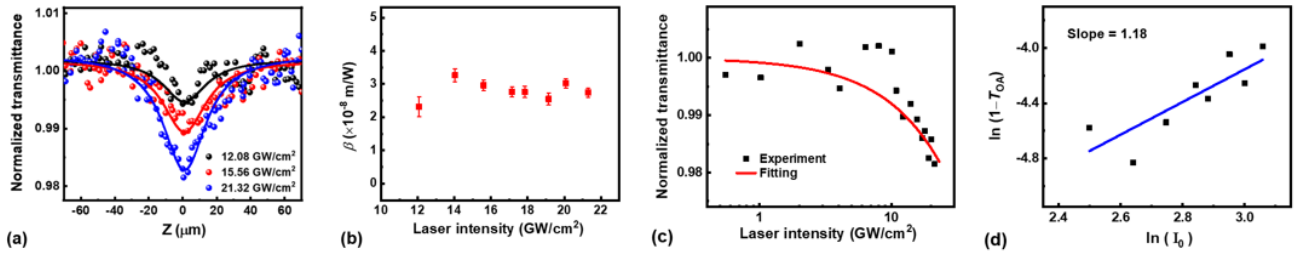

Figure 3. (a) OA Z-scan results of $PdSe_2$ film at different intensities. (b) TPA coefficient β of $PdSe_2$ film versus laser intensity. (c) Normalized transmittance of $PdSe_2$ film at the focal point as a function of laser intensity. (d) The plot of $\ln(1-T_{OA})$ versus $\ln(I_0)$ to determine the order of nonlinearity. The measured and fit results are shown by scatter data points and solid lines, respectively.

To further investigate the nonlinear absorption of the $PdSe_2$ film, we measured the minimum transmittance with the sample at the focal point of the Z scan setup, for different incident laser intensities. Figure 3(c) shows the transmittance of

Preprints (www.preprints.org) | NOT PEER-REVIEWED | Posted: 1 March 2021 doi:10.20944/preprints202103.0021.v1

$PdSe_2$ at the focal point as a function of laser intensity, where the transmittance fluctuates around a relatively constant value at low intensities and then decreases significantly as the laser intensity increased. The experimental data fits the theory well, [31] verifying our assumption of TPA being the dominant process for nonlinear absorption in the $PdSe_2$ film. The order of the observed nonlinear absorption can also be confirmed by examining the relation between $\ln(1-T_{OA})$ versus $\ln(I_0)$: [32]

$$\ln(1 - T_{OA}) = k\ln(I_0) + C, \quad (1)$$

where k is the slope showing the order of the nonlinear absorption and C is a constant. For pure TPA, the slope is equal to 1. [32] We obtain a slope of 1.18 (Figure 3(d)), suggesting the observed nonlinear absorption is mainly attributed to TPA in the $PdSe_2$ film.

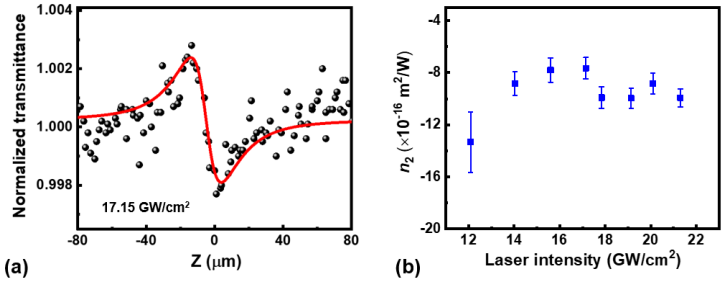

Figure 4. (a) Representative CA Z-scan result of $PdSe_2$ film at intensity of 17.15 GW/cm^2. (b) Kerr coefficient n_2 of $PdSe_2$ film versus laser intensity.

We also performed CA Z-scan measurements to investigate the Kerr nonlinearity (n_2) of the $PdSe_2$ films. The values of n_2 for the $PdSe_2$ film at different laser intensities were extracted by fitting the measured CA results. Figure 4(a) shows a representative CA result for $PdSe_2$ at a laser intensity of 17.15 GW/cm^2. The transmittance of the sample exhibited a transition from peak to valley when the sample passed through the focal plane. Such a peak-valley CA behaviour corresponds to a negative Kerr coefficient n_2 and indicates an optical self-defocusing effect in the $PdSe_2$ film. The noise in the CA data is mainly induced by the light scattering in the $PdSe_2$ film surface. By improving the film uniformity, such noise can be further reduced. As discussed above, TPA results in the transfer of electrons from valence band to conduction band, increasing the free carrier density in the film. Therefore, the observed negative Kerr nonlinearity potentially originates from the TPA-induced free carrier nonlinear refraction and interband blocking. [33,34]

Figure 4(b) shows the measured Kerr coefficient n_2 of $PdSe_2$ versus laser intensity, showing a large n_2 of -1.33×10^{-15} m^2/W. Table 1 compares the β and n_2 of $PdSe_2$ with other 2D layered materials. As can be seen, the value of n_2 for $PdSe_2$ is lower than those of graphene and GO, but still more than two orders of magnitude higher than bulk silicon. [35,36] Such a high n_2 suggests that $PdSe_2$ is an extremely promising material for self-defocusing based nonlinear photonic applications. For example, a negative Kerr nonlinearity can be used to self-compress ultrashort pulses in the presence of positive group-velocity dispersion. [37] Another application of a negative Kerr nonlinearity is mode locking of lasers using the Kerr mode-locking technique [35,38] as well as the possibility of achieving net parametric modulational instability gain under normal dispersion conditions. [35,39]

In addition, as shown in Figure 4(b), the absolute value of n_2 initially decreases with laser intensity and then saturates at higher intensities. In theory, the optical nonlinear refraction originates mainly from the free-carrier and bound-electron nonlinearities. [33,40-44] We assume that the two mechanisms co-exist in the $PdSe_2$ film. It has been shown that, near the half-bandgap the two-photon resonance typically yields a positive n_2. However, at higher photon energies, the bound-electron contribution to the n_2 nonlinearity becomes negative, while the free-carrier nonlinearity is usually also negative. [33,44] We therefore infer that either, or both, processes contribute to the nonlinearity since we observed a negative Kerr nonlinearity for the $PdSe_2$ film. This is further complicated by the fact that $PdSe_2$ is an indirect bandgap material. The Kerr nonlinearity is dominated by direct transitions at all energies, whereas the nonlinear absorption is dominated by indirect transitions in energy regions where the direct transitions are not allowed (eg., below half of the direct bandgap for TPA). [45]

The refractive index change in the $PdSe_2$ film can be expressed by $\Delta n = n_2^* I_0 + \sigma_r N$, where n_2^* is the nonlinear refraction related to bonding electrons, σ_r is the free carrier refractive coefficient and N is the charge carrier density. [33] Therefore, the effective $n_2 = \Delta n/I_0 = n_2^* + \sigma_r N/I_0$, is an intensity dependent parameter, which can explain the n_2 variation as a function of laser intensity observed in our measurements.

Preprints (www.preprints.org) | NOT PEER-REVIEWED | Posted: 1 March 2021 doi:10.20944/preprints202103.0021.v1

Table 1. Comparison of β and n_2 for various 2D layered materials

Material	Laser parameter	Thickness	β (m/W)	n_2 (m^2/W)	n_2 (×n_2 of Si[1])	Ref.
Graphene	1150 nm, 100 fs	5-7 layers	3.8×10^{-8}	-5.5×10^{-14}	-1.22×10^{4}	[42]
GO	800 nm, 100 fs	~2 μm	4×10^{-7}	1.25×10^{-13}	2.75×10^{4}	[29]
MoS_2	1064 nm, 25 ps	~25 μm	$(-3.8 \pm 0.59) \times 10^{-11}$	$(1.88 \pm 0.48) \times 10^{-16}$	41.32	[11]
WS_2	1040 nm, 340 fs	~57.9 nm	$(1.81 \pm 0.08) \times 10^{-8}$	$(-3.36 \pm 0.27) \times 10^{-16}$	-73.85	[12]
BP	1030 nm, 140 fs	~15 nm	5.845×10^{-6}	-1.635×10^{-12}	-3.59×10^{5}	[14]
$PtSe_2$	800 nm, 150 fs	~4.6 nm	-8.80×10^{-8}	–	–	[43]
$PtSe_2$	1030 nm, 340 fs	17 layers	–	$(-3.76 \pm 0.46) \times 10^{-15}$	-8.26×10^{2}	[32]
$PdSe_2$	800 nm, 140 fs	~8 nm	$(3.26 \pm 0.19) \times 10^{-8}$	$(-1.33 \pm 0.23) \times 10^{-15}$	-2.92×10^{2}	This work

[1] n_2 for silicon = 4.55×10^{-18} m^2/W (ref. [36])

4. CONCLUSION

In summary, we report a large third-order nonlinear optical response of $PdSe_2$ films measured with the Z-scan technique. Experimental results show that $PdSe_2$ has a strong TPA response with a large β of ~ 3.26×10^{-8} m/W. The Kerr nonlinearity (n_2) of $PdSe_2$ is also investigated. We find that n_2 is negative, and with an absolute magnitude that is more than two orders of magnitude larger than bulk silicon. Furthermore, we characterize the variation in n_2 of $PdSe_2$ with laser intensity, finding that n_2 initially increases (decreasing in absolute magnitude) with incident laser intensity and then saturates at higher intensities. Our results verify $PdSe_2$ as a promising 2D material with prominent nonlinear optical properties.

ACKNOWLEDGEMENT

This work was supported by the Australian Research Council Discovery Projects Program (No. DP150102972 and DP190103186), and the Industrial Transformation Training Centres scheme (Grant No. IC180100005). We acknowledge Swinburne Nano Lab and Micro Nano Research Facility (MNRF) of RMIT University for the support in material characterization as well as Shenzhen Sixcarbon Technology for the $PdSe_2$ film fabrication. We thank Dr. Yunyi Yang and Dr. Tania Moein for technical support, Dr. Deming Zhu for assisting in XPS characterization and Dr. Chenglong Xu for assisting in optical characterization.

REFERENCES

[1] Lim, G.-K.; Chen, Z.-L.; Clark, J.; Goh, R. G. S.; Ng, W.-H.; Tan, H.-W.; Friend, R.H.; Ho, P. K. H.; Chua, L.-L. Giant broadband nonlinear optical absorption response in dispersed graphene single sheets. *Nat. Photonics* 2011, *5*, 554-560.

[2] Pan, T.; Qiu, C.; Wu, J.; Jiang, X.; Liu, B.; Yang, Y.; Zhou, H.; Soref, R.; Su, Y. Analysis of an electro-optic modulator based on a graphene-silicon hybrid 1D photonic crystal nanobeam cavity. *Opt. Express* 2015, *23*, 23357-233364.

[3] Wu, J., Jia, L., Zhang, N., Qu, Y., Jia, B. and Moss, D. J. Graphene Oxide for Integrated Photonics and Flat Optics. *Adv. Mater.* **2020**, 32, 1-29, 2006415.

[4] Yang, Y.; Wu, J.; Xu, X.; Liang, Y.; Chu, S. T.; Little, B. E.; Morandotti, R.; Jia, B.; Moss, D. J. Invited Article: Enhanced four-wave mixing in waveguides integrated with graphene oxide. *APL Photonics* 2018, 3, 120803.

[5] Yang, Y.; Lin, H.; Zhang, B. Y.; Zhang, Y.; Zheng, X.; Yu, A.; Hong, M.; Jia, B. Graphene-based multilayered metamaterials with phototunable architecture for on-chip photonic devices. *ACS Photonics* 2019, 6, 1033-1040.

[6] Wu, J.; Yang, Y.; Qu, Y.; Xu, X.; Liang, Y.; Chu, S. T.; Little, B. E.; Morandotti, R.; Jia, B.; Moss, D. J. Graphene oxide waveguide and micro-ring resonator polarizers. *Laser Photonics Rev.* 2019, 13, 1900056.

[7] Wu, J.; Yang, Y.; Qu, Y.; Jia, L.; Zhang, Y.; Xu, X.; Chu, S. T.; Little, B. E.; Morandotti, R.; Jia, B.; Moss, D. J. 2D Layered graphene oxide films integrated with micro-ring resonators for enhanced nonlinear optics. *Small* 2020, 16, 1906563.

[8] Zhang, Y.; Wu, J.; Yang, Y.; Qu, Y.; Jia, L.; Moein, T.; Jia, B.; Moss, D. J. Enhanced Kerr Nonlinearity and Nonlinear Figure of Merit in Silicon Nanowires Integrated with 2D Graphene Oxide Films. *ACS Appl. Mater. Interfaces* 2020, 12, 33094-33103.

[9] Qu, Y., Wu, J., Yang, Y., Zhang, N., Liang, Y., Dirani, H. E., Crochemore, R., Demongodin, P., Sciancalepore, C., Grillet, C., Monat, C., Jia, B., David J. Moss. Enhanced Four-Wave Mixing in Silicon Nitride Waveguides Integrated with 2D Layered Graphene Oxide Films. *Adv. Opt. Mater.* 2020, 8, 2001048.

[10] Chen, H.; Corboliou, V.; Solntsev, A. S.; Choi, D. Y.; Vincenti, M. A.; de Ceglia, D.; de Angelis, C.; Lu, Y.; Neshev, D. N. Enhanced second-harmonic generation from two-dimensional $MoSe_2$ on a silicon waveguide. *Light: Science & Applications* 2017, *6*, e17060.

[11] Bikorimana, S.; Lama, P.; Walser, A.; Dorsinville, R.; Anghel, S.; Mitioglu, A.; Micu, A.; Kulyuk, L. Nonlinear optical response in two-dimensional transition metal dichalcogenide multilayer: WS2, WSe2, MoS2 and Mo0.5W0.5S2. *Opt. Express* 2016, 24, 20685-20695.

[12] Dong, N.; Li, Y.; Zhang, S.; McEvoy, N.; Zhang, X.; Cui, Y.; Zhang, L.; Duesberg, G. S.; Wang, J. Dispersion of nonlinear refractive index in layered WS2 and WSe2 semiconductor films induced by two-photon absorption. *Opt. Lett.* 2016, 41, 3936-3939.
[13] Zheng, X.; Chen, R.; Shi, G.; Zhang, J.; Xu, Z.; Cheng, X.; Jiang, T. Characterization of nonlinear properties of black phosphorus nanoplatelets with femtosecond pulsed Z-scan measurements. *Opt. Lett.* 2015, *40*, 3480.
[14] Yang, T.; Abdelwahab, I.; Lin, H.; Bao, Y.; Tan, S. J. R.; Fraser, S.; Loh, K. P.; Jia, B. Anisotropic third-order nonlinearity in pristine and lithium hydride intercalated black phosphorus *ACS Photonics* 2018, *5*, 4969-4977.
[15] Chen, B.; Zhang, X.; Wu, K.; Wang, H.; Wang, J.; Chen, J. Q-switched fiber laser based on transition metal dichalcogenides MoS_2, $MoSe_2$, WS_2, and WSe_2. *Opt. Express* **2015**, *23*, 26723-26737.
[16] Du, L.; Jiang, G.; Miao, L.; Huang, B.; Yi, J.; Zhao, C.; Wen, S. Few-layer rhenium diselenide: an ambient-stable nonlinear optical modulator. *Opt. Mater. Express* 2018, 8, 926-935.
[17] Zhang, C.; Ouyang, H.; Miao, R.; Sui, Y.; Hao, H.; Tang, Y.; You, J.; Zheng, X.; Xu, Z.; Cheng, X.; Jiang, T. Anisotropic nonlinear optical properties of a SnSe flake and a novel perspective for the application of all-optical switching. *Adv. Opt. Mater.* 2019, *7*, 1900631.
[18] Oyedele, A. D.; Yang, S.; Liang, L.; Puretzky, A. A.; Wang, K.; Zhang, J.; Yu, P.; Pudasaini, P. R.; Ghosh, A. W.; Liu, Z.; Rouleau, C. M.; Sumpter, B. G.; Chisholm, M. F.; Zhou, W.; Rack, P. D.; Geohegan, D. B.; Xiao, K. $PdSe_2$: Pentagonal two-dimensional layers with high air stability for electronics. *J. Am. Chem. Soc.* 2017, *139*, 14090-14097.
[19] Zhang, G.; Amani, M.; Chaturvedi, A.; Tan, C.; Bullock, J.; Song, X.; Kim, H.; Lien, D.-H.; Scott, M. C.; Zhang, H.; Javey, A. Optical and electrical properties of two-dimensional palladium diselenide. *Appl. Phys. Lett.* 2019, *114*, 253102.
[20] Jiang, S.; Xie, C.; Gu, Y.; Zhang, Q.; Wu, X.; Sun, Y.; Li, W.; Shi, Y.; Zhao, L.; Pan, S.; Yang, P.; Huan, Y.; Xie, D.; Zhang, Q.; Liu, X.; Zou, X.; Gu, L.; Zhang, Y. Anisotropic growth and scanning tunneling microscopy identification of ultrathin even layered $PdSe_2$ ribbons. *Small* 2019, *15*, 1902789.
[21] Jia, L., Wu, J., Yang, T., Jia, B., Moss, D. J. Large Third-Order Optical Kerr Nonlinearity in Nanometer-Thick $PdSe_2$ 2D Dichalcogenide Films: Implications for Nonlinear Photonic Devices. *ACS Appl. Nano Mater.* 2020, 3, 6876-6883.
[22] Liang, Q.; Wang, Q.; Zhang, Q.; Wei, J.; Lim, S. X.; Zhu, R.; Hu, J.; Wei, W.; Lee, C.; Sow, C.; Zhang, W.; Wee, A. T. S. High-Performance, room temperature, ultra-broadband photodetectors based on air-stable $PdSe_2$. *Adv. Mater.* 2019, *31*, 1807609.
[23] Zeng, L.-H.; Wu, D.; Lin, S.-H.; Xie, C.; Yuan, H.-Y.; Lu, W.; Lau, S. P.; Chai, Y.; Luo, L.-B.; Li, Z.-J.; Tsang, Y. H. Controlled synthesis of 2D $PdSe_2$ for sensitive photodetector applications. *Adv. Funct. Mater.* 2019, *29*, 1806878.
[24] Ma, Y.; Zhang, S.; Ding, S.; Liu, X.; Yu, X.; Peng, F.; Zhang, Q. Passively Q-switched Nd: $GdLaNbO_4$ laser based on 2D $PdSe_2$ nanosheet. *Optics and Laser Technology*, 2019, *124*, 105959.
[25] Zhang, H.; Ma, P.; Zhu, M.; Zhang, W.; Wang, G.; Fu, S. Palladium selenide as a broadband saturable absorber for ultra-fast photonics. *Nanophotonics* 2020, https://doi.org/10.1515/nanoph-2020-0116.
[26] Xu, H.; Zhang, H.; Liu, Y.; Zhang, S.; Sun, Y.; Guo, Z.; Sheng, Y.; Wang, X.; Luo, C.; Wu, X.; Wang, J.; Hu, W.; Xu, Z.; Sun, Q.; Zhou, P.; Shi, J.; Sun, Z.; Zhang, D. W.; Bao, W. Controlled doping of wafer-scale $PtSe_2$ films for device application. *Adv. Funct. Mater*. 2019, *29*, 1805614.
[27] Jia, L.; Cui, D.; Wu, J.; Feng, H.; Yang, Y.; Yang, T.; Qu, Y.; Du, Y.; Hao, W.; Jia, B.; Moss, D. J. Highly nonlinear BiOBr nanoflakes for hybrid integrated photonics. *APL Photonics* 2019, *4*, 090802.
[28] Sheik-Bahae, M.; Said, A. A.; Wei, T.-H.; Hagan, D. J.; Stryland, E. W. V. Sensitive measurement of optical nonlinearities using a single beam. *IEEE J. Quantum Electron*. 1990, *26*, 760-769.
[29] Zheng, X.; Jia, B.; Chen, X.; Gu, M. In situ third-order nonlinear responses during laser reduction of graphene oxide thin films towards on-chip nonlinear photonic devices. *Adv. Mater.* 2014, *26*, 2699-2703.
[30] Chantharasupawong, P.; Philip, R.; Narayanan, N. T.; Sudeep, P. M.; Mathkar, A.; Ajayan, P. M.; Thomas, J. Optical power limiting in fluorinated graphene oxide: an insight into the nonlinear optical properties. *J. Phys. Chem. C* 2012, *116*, 25955-25961.
[31] Wang, G.; Bennett, D.; Zhang, C.; Ó Coileáin, C.; Liang, M.; McEvoy, N.; Wang, J. J.; Wang, J.; Wang, K.; Nicolosi, V.; Blau, W. J. Two-photon absorption in monolayer MXenes. *Adv. Opt. Mater*. 2020, *8*, 1902021.
[32] Wang, L.; Zhang, S.; McEvoy, N.; Sun, Y.; Huang, J.; Xie, Y.; Dong, N.; Zhang, X.; Kislyakov, I. M.; Nunzi, J. M.; Zhang, L.; Wang, J. Nonlinear optical signatures of the transition from semiconductor to semimetal in $PtSe_2$. *Laser Photonics Rev*. 2019, *13*, 1900052.
[33] Hagan, D. J.; Van Stryland, E. W.; Soileau, M. J.; Wu, Y. Y. Self-protecting semiconductor optical limiters. *Opt. Lett*., 1988, *13*, 315-317.
[34] Said, A. A.; Sheik-Bahae, M.; Hagan, D. J.; Wei, T. H.; Wang, J.; Young, J.; Van Stryland, E. W. Determination of bound-electronic and free-carrier nonlinearities in ZnSe, GaAs, CdTe, and ZnTe. *J. Opt. Soc. Am. B* 1992, *9*, 405-414.
[35] Pasquazi, A.; Peccianti, M.; Razzari, L.; Moss, D. J.; Coen, S.; Erkintalo, M.; Chembo, Y. K.; Hansson, T.; Wabnitz, S.; Del'Haye, P.; Xue, X.; Weiner, A. M.; Morandotti, R. Micro-Combs: A Novel Generation of Optical Sources. *Physics Reports* 2018, *729*, 1-81.
[36] Moss, D. J.; Morandotti, R.; Gaeta, A. L.; Lipson, M. New CMOS-compatible platforms based on silicon nitride and Hydex for nonlinear optics. *Nat. Photonics* 2013, *7*, 597-607.
[37] DeSalvo, R.; Hagan, D. J.; Sheik-Bahae, M.; Stegeman, G.; Van Stryland, E. W.; Vanherzeele, H. Self-focusing and self-defocusing by cascaded second-order effects in KTP. *Opt. Lett*. 1992, *17*, 28-30.
[38] Kriso, C.; Kress, S.; Munshi, T.; Grossmann, M.; Bek, R.; Jetter, M.; Michler, P.; Stolz, W.; Koch, M.; Rahimi-Iman, A. Microcavity-enhanced Kerr nonlinearity in a vertical-external-cavity surface-emitting laser. *Opt. Express* 2019, *27*, 11914-11929.

 doi:10.20944/preprints202103.0021.v1

[39] Liu, Y.; Xuan, Y.; Xue, X.; Wang, P.-H.; Chen, S.; Metcalf, A. J.; Wang, J.; Leaird, D. E.; Qi, M.; Weiner, A. M. Investigation of mode coupling in normal-dispersion silicon nitride microresonators for Kerr frequency comb generation. *Optica* 2014, *1*, 137-144.
[40] Lu, S.; Zhao, C.; Zou, Y.; Chen, S.; Chen, Y.; Li, Y.; Zhang, H.; Wen, S.; Tang, D. Third order nonlinear optical property of Bi_2Se_3. *Opt. Express* 2013, *21*, 2072-2082.
[41] Sheik-Bahae, M.; Hagan, D. J.; Van Stryland, E. W. Dispersion of bound electronic nonlinear refraction in solids. *IEEE J. Quantum Electron*. 1991, *27*, 1296-1309.
[42] Demetriou, G.; Bookey, H. T.; Biancalana, F.; Abraham, E.; Wang, Y.; Ji, W.; Kar, A. K. Nonlinear optical properties of multilayer graphene in the infrared. *Opt. Express* 2016, *24*, 13033-13043.
[43] Wang, G.; Wang, K.; McEvoy, N.; Bai, Z.; Cullen, C. P.; Murphy, C. N.; McManus, J. B.; Magan, J. J.; Smith, C. M.; Duesberg, G. S.; Kaminer, I.; Wang, J.; Blau, W. J. Ultrafast carrier dynamics and bandgap renormalization in layered $PtSe_2$. *Small* 2019, *15*, 1902728.
[44] Huang, J.; Dong, N.; McEvoy, N.; Wang, L.; Coileain, C. O.; Wang, H.; Cullen, C. P.; Chen, C.; Zhang, S.; Zhang, L.; Wang, J. Surface-State Assisted Carrier Recombination and Optical Nonlinearities in Bulk to 2D Nonlayered PtS. *ACS Nano* 2019, *13*, 13390.
[45] Moss, D. J.; Ghahramani, E.; Sipe, J. E.; van Driel, H. M. Band structure calculation of dispersion and anisotropy in $\chi(3)$ for third harmonic generation in Si, Ge, and GaAs. *Phys. Rev. B* 1990, *41*, 1542-1560.